

A Unified Object Counting Network with Object Occupation Prior

Shengqin Jiang, Qing Wang, Fengna Cheng, Yuankai Qi, Qingshan Liu, *IEEE Senior Member*

Abstract—The counting task, which plays a fundamental role in numerous applications (e.g., crowd counting, traffic statistics), aims to predict the number of objects with various densities. Existing object counting tasks are designed for a single object class. However, it is inevitable to encounter newly coming data with new classes in our real world. We name this scenario as *evolving object counting*. In this paper, we build the first evolving object counting dataset and propose a unified object counting network as the first attempt to address this task. The proposed model consists of two key components: a class-agnostic mask module and a class-increment module. The class-agnostic mask module learns generic object occupation prior via predicting a class-agnostic binary mask (e.g., 1 denotes there exists an object at the considering position in an image and 0 otherwise). The class-increment module is used to handle new coming classes and provides discriminative class guidance for density map prediction. The combined outputs of class-agnostic mask module and image feature extractor are used to predict the final density map. When new classes come, we first add new neural nodes into the last regression and classification layers of this module. Then, instead of retraining the model from scratch, we utilize knowledge distilling to help the model remember what have already learned about previous object classes. We also employ a support sample bank to store a small number of typical training samples of each class, which are used to prevent the model from forgetting key information of old data. With this design, our model can efficiently and effectively adapt to new coming classes while keeping good performance on already seen data without large-scale retraining. Extensive experiments on the collected dataset demonstrate the favorable performance.

Index Terms—Object counting, Incremental learning, Classification, Convolution neural network.

I. INTRODUCTION

IN order to analyze crowded scenarios, object counting aims to automatically estimate the number of targets in an image or a video frame [1], [2]. With the continuous growth of crowding scenarios and the increasing demand for production automation, this task has received extensive attention in academia and industry. Its applications cover a variety of domains, including traffic management, smart agriculture and public safety monitoring.

Crowd counting, as a specific application of object counting, has been well explored so far due to the prevalence of high-

density scenes in public areas, gatherings and other events. In particular, the outbreak of COVID-19 [3] in recent years has highlighted its importance and practicality. To properly forecast the number of targets, it is important to overcome a variety of challenging, including extreme occlusion, scale variation and clutter background. To address these issues, [4] leveraged heterogeneous auxiliary tasks including attentive crowd segmentation, distilled depth prediction and crowd count regression to assist crowd counting. [5] addressed scale variation of pedestrians in a crowd image with the help of depth-embedded convolutional neural networks. [6] investigated several methods for incorporating the object/non-object mask into the regression of the density map. [7] used high-level semantic information to serve as a guide and constraint for generating high-quality density maps. [8] proposed an effective counting network with lightweight design in encoding and decoding phases. These studies have considerably increased the performance of network prediction, which boosts the development of this field.

Actually, the requirements for this task are widespread in real scenarios. For example, [9] put forward a novel FCN-rLSTM network to jointly estimate vehicle density and vehicle count. [10] counted multi-scale and dense wheat heads in a wild environment with data augmentation. [11] developed a neural network deployed in Android to detect kiwifruits for yield estimation. This indicates that the classes required in real application scenarios are dynamic. However, the above works make it simple to conclude that the efforts are done to explore the counting of a specific class, which is difficult to perceive multiple classes incrementally. One straightforward solution to this is training all the classes together. Even though this method can accurately predict each class, getting the final prediction model demands a lot of hardware resources and costs when the number of data increases exponentially. An alternative solution is fine-tuning. The old classes are easy to forget, despite the fact that we can learn a new model for new class with satisfied accuracy. What needs special attention is that the difficulty gets worse as the number of classes grows. This raises the question of how to incrementally learn the expanding classes for object counting while retaining old knowledge.

To address this challenge, we propose a unified object counting network that can take in a stream of data with various classes occurring constantly at different times. The proposed network consists of three parts: base net, class-agnostic mask module and class-increment module. This design not only ensures that the network can dynamically learn new data with new classes, but it also strengthens the network prediction abil-

Manuscript received December *** **; revised *** **, 2022. (*Corresponding author: Qingshan Liu, Yuankai Qi.*)

S. Jiang, Q. Wang, Q. Liu are with the School of Computer and Software, Nanjing University of Information Science and Technology, Nanjing, 210044, China (e-mail: {jiangshengmeng@126.com, 20211249453@nuist.edu.cn, qslu@nuist.edu.cn}).

F. Cheng is with College of Mechanical and Electronic Engineering, Nanjing Forestry University, Nanjing, 210037, China (e-mail: cfn1218@163.com)

Y. Qi is with Australian Institute for Machine Learning, the University of Adelaide, Adelaide, SA 5005, Australia (e-mail: qyqshr@gmail.com).

ities by utilizing object occupation prior. Without retraining the network from scratch, we train the network with newly added data with new classes. Further, we employ knowledge distilling and support sample bank to alleviate the problem of catastrophic forgetting. Finally, extensive experiments are conducted to demonstrate the effectiveness of our model, and we achieve state-of-the-art performance with other recent methods. The main contributions are summarized as follows:

(1) We propose a unified network framework for evolving object counting. To the best of our knowledge, this is the first attempt to incrementally learn different classes of this task. To achieve such a challenging task, we additionally collect a sizable evolving object counting dataset named EoCo with 6885 samples.

(2) The class-incremental module is put forward to dynamically expand the final regressor layer of class-related density map according to the newly added class. The regressor achieves its own optimization and the selection of the density map via the guidance of the incremental classifier.

(3) The class-agnostic mask module improves the perception ability of network for interest targets and background regions by disregarding class information. By introducing the network generic object occupation prior, it makes density regression less challenging.

(4) Extensive experiments on EoCo dataset show the validity of our strategies, and we achieve superior performance compared to recent existing methods.

II. RELATED WORK

Object Counting. The goal of object counting is to produce an accurate number prediction for images of varying densities. It is valuable in the field of public place safety management, traffic flow monitoring, and smart agriculture [12], [13]. To better comprehend the evolution of this task, we trace the progress from the perspective of crowd counting. Generally, crowd counting models can be divided into two types: traditional methods and deep learning based methods. The traditional methods include detection-based approaches [14], [15] and regression-based approaches [16], [17]. For example, [18] proposed two steps for estimating the number of people in crowded scenes with perspective transformation, that is, recognition of the head-like contour and estimation of crowd size. [19] built the mixtures of multiscale deformable part models for robust object detection. Differently, [17] utilized Gaussian Process regression to learn a mapping between the extracted features and the number of people per segment of the crowd. Yet, the limited power of handcraft features to characterize objects makes it difficult to generalize them.

Thanks to the excellent performance of convolutional neural networks (CNNs) in image classification, several efforts have been devoted to explore its extensions in this field [20]. As one of the earliest CNN-based works, [21] trained the deep model to predict crowd density and count in a switchable learning procedure. Unfortunately, when the crowd is too dense, it is easy to lead to difficulties in network optimization directly through linear regression. To address this issue, [22] proposed using the density map produced by Gaussian kernel instead

of directly estimating the number of crowd. Meanwhile, the authors also designed a multi-column CNN with different receptive field to solve the scale variation. Further, by deliberately combining global and local contextual information, CP-CNN [23] aimed to produce high-quality crowd density and count estimation. After that, CSRNet [24] explored a straightforward and efficient single column structure in contrast to these sophisticated multi-column network designs. Specially, it used pre-trained VGG-16 [25] as backbone and stacked dilated convolutions as backend. [26] studied a zooming mechanism for crowd counting in low to high density scenarios. P2PNet [27] exploited a purely point-based network framework for joint crowd counting and individual localization instead of predicting a density map. CCTrans [28] employed vision transformer as the backbone with multi-scale receptive fields for predicting the final results. More recently, CDANet [29] built a cross-domain attention network to explore the unlabeled domain on both unsupervised synthetic-to-realistic and realistic-to-realistic crowd counting. FLCB [30] studied a counting task for continuously learning with the new domain data in real scenarios rather than fitting only one domain.

Counting different types of objects, in addition to crowd counting, is a widely used technique, particularly in transportation and agriculture. [9] proposed to jointly estimate vehicle density and vehicle count by combining CNNs with LSTM in a residual learning fashion. As for the field of agriculture, [31] combined deep learning models with conventional 3D processing methods to develop a pipeline for fast and precise SLAM for grape counting. [32] proposed using a semantic segmentation regression network to count wheat ears in remote images. [33] utilized an image processing-based technique to automatically count and classify *Rhopalosiphum padi*. These studies emphasize the importance of object counting in a variety of fields, as well as the fact that the class of targets varies constantly in real-world applications. These methods generally learn a mapping for a single class. This means that when the classes change, it is necessary to retrain the network parameters or transfer knowledge. Obviously, these methods cannot learn the counting for dynamic object classes online, which limits the flexibility and universality of deep models.

Class Incremental Learning. Generally, incremental learning refers to a learning system which has the ability to continuously learn the new class from fresh samples while retaining the majority of previously taught knowledge [34], [35]. Nevertheless, catastrophic forgetting, or the inability to recall prior knowledge while acquiring new skills, is a serious challenge in the dynamic learning process. Consequently, a variety of techniques are exploited to address the issue from various perspectives, such as regularization, knowledge replay and parameter isolation. LwF [36] is an example of a regularization strategy that imposes constraints on the loss functions of new tasks to prevent knowledge from covering them. To do this, it combined standard cross-entropy loss with distillation loss. These techniques seldom ever require old data to remember historical information without jeopardizing privacy. Different from them, iCaRL [37] replayed old knowledge by reviewing a small number of representative

exemplars, known as knowledge replay. These exemplars are selected close to the class center with given fixed number. Since then, various methods have investigated the method in further detail. As for parameter isolation, [38] observed each example just once, and hyper-parameter selection is carried out on a limited number and disjoint set of tasks that are not used for the real learning process and evaluation. The majority of methods concentrate on tasks like classification [37] and segmentation [39], but they seldom ever include regression tasks like object counting.

III. PROBLEM FORMULATION

This section presents the problem setting of class incremental learning of object counting. Before that, we will first go through a specific class, crowd counting, to better comprehend the main objective. There is a dataset $D = \{x_i, y_i, i = 1, 2, \dots, m\}$, where x_i and y_i denote the input image and dot-annotation label, respectively. The label y_i is then transformed to density map via Gaussian kernel as the newly generated image label [22]. To learn the map between inputs and labels, a network model $Net(x, \theta)$ is built with learnable parameters θ . It is composed of a feature extractor $f(x, \vartheta)$ and a regressor $g(\gamma|\vartheta)$ with $\theta = \{\vartheta, \gamma\}$. The network parameters are optimized via MSE loss:

$$\mathcal{L} = \frac{1}{2n} \sum_{i=1}^n \|Net(x_i, \theta) - y_i\|_2^2, \quad (1)$$

The purpose of this study is to continually learn how to count the inputs from a new class without forgetting or degrading too much on previously taught ones. In other words, the well-trained network achieves better trade-off between stability and plasticity. Without losing generality, assume that there is a dataset D_{total} with D^{tr} for training and D^{test} for test, each of which is a member of the class set $\mathcal{C} = \{c_0, c_1, \dots, c_k\}$. Note that there are k counting classes and one background denoted by c_0 . The reason for this setting is that it prevents incorrect prediction by classifying samples that do not fit into one of the k classes as background.

Based on the above setting, the network has learned the training sets from D_1^{tr} to D_{t-1}^{tr} after it has learned the first $t-1$ classes. The preceding $t-1$ classes is now known as the old classes while learning the t th class, and $(\bigcup_{i=1}^{t-1} D_i^{tr}) \cap D_t^{tr} = \emptyset$. It should be noticed that the background samples are trained together with the 1st-class ones. After t rounds of training, the network is expected to count any samples from the learned classes well.

IV. OUR MODEL

Unlike incremental tasks such as image classification [40] and semantic segmentation [41], there is no explicit class information for object counting, making it difficult to simply adapt the existing incremental learning model to this problem. To this end, we propose a unified network framework for evolving object counting termed as EoCNet.

The overview of the k -th incremental step of EoCNet for object counting is illustrated in Fig. 1. We use the first ten

layers of VGG-16 as the network backbone to extract features. To robustly achieve incremental learning at step t , the following components are designed: class-incremental module, class-agnostic mask module and representative counting memory. In what follows, we will go over each of these three components in further details.

A. Class-Incremental Module

This module aims to dynamically extend the feature representation to be compatible with the growing number of classes. To achieve such a goal, we build a dynamical expandable 1×1 convolution learning representation when encountering new classes. Specifically, at step t , $t+1$ convolution kernels are built in which the initialization of the first t kernel parameters inherits from the parameters learned from the $t-1$ old classes (including background), and the newly added kernel are randomly initialized. Obviously, we can dynamically expand the prediction of density maps, such that different classes have independent count outputs. If the class does not exist, it will be classified as background. However, there is an evident issue here that is also distinct from the conventional incremental classification task. That is, even if we explicitly set the density map to be sorted by class, there may exist values in different channels of the predicted density maps. As a result, it is challenging to determine which density map should be the output of this image if the network predictions are influenced by noises.

To this end, we propose a classifier guided learning strategy which allows the network to learn the class of inputs and dynamically pick the network output depending on the classification information. To be more specific, we first build a simple class classifier, that is, we feed the output of feature extractor $f(x, \vartheta)$ into an average pooling layer before making the final prediction with a linear layer. This branch is optimized by the cross entropy loss as below:

$$\mathcal{L}_c = -\frac{1}{M} \sum_{i=1}^M y_i \log(p_i), \quad (2)$$

where y_i is the ground truth of object class, p_i denotes the prediction result by the classifier, \tilde{D}_t^{tr} and M denote the training set and the number of samples, respectively.

Then the learning of density map with multiple classes is defined as follows:

$$\mathcal{L}_d = \frac{1}{2n} \sum_{i=1}^n \sum_{j=1}^t (\hat{p}_i == j) \left\| Net(x_i, \theta)_i^j - y_i^j \right\|_2^2, \quad (3)$$

where $\hat{p}_i = \text{argmax}(p_i)$. In this manner, we dynamically learn and forecast the density map based on the prediction of class classifier. Note that the last linear layer of the class classifier is constantly enlarged when a new class is encountered.

B. Class-agnostic Mask Module

Class-agnostic mask module is utilized to provide a generic object occupation prior for the objects from all the classes, which can improve the extraction of region of interest without

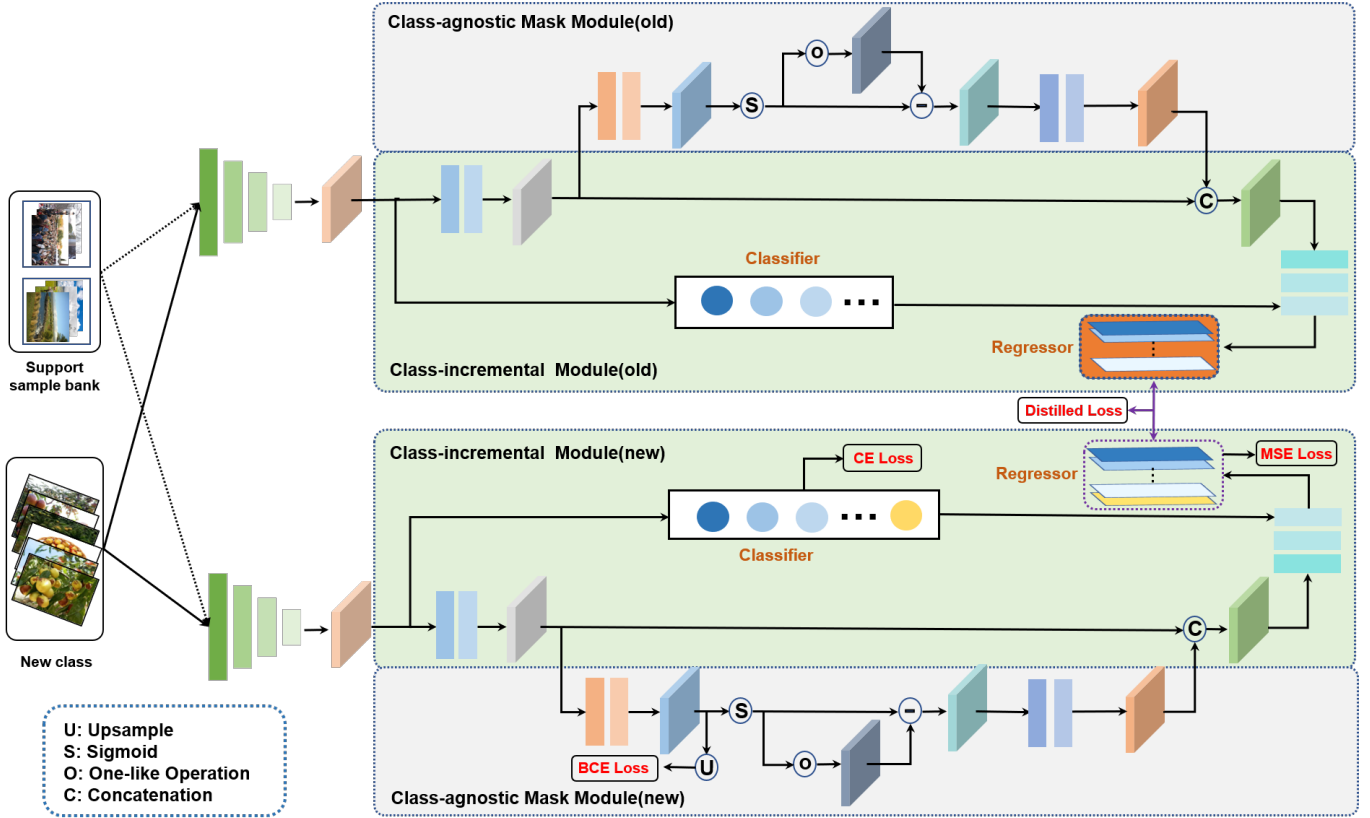


Fig. 1. Overview of the k -th incremental step of EoCNet for object counting. CE loss, BCE loss and MSE loss denote cross entropy loss, binary cross entropy loss and mean squared error, respectively.

dynamically growing the network and lessen the difficulties of network regression. Another advantage is that this setting avoids incrementally setting the convolution kernels of the module, reducing tedious settings and complex operations. For this purpose, we employ a class-agnostic binary representation of density map as a supervision. Specially, through a sequence of convolution processes, we obtain a transformed feature from the output of the feature extractor $f(x, \vartheta)$. Then, using a 1×1 convolution and sigmoid operation, a pixel-level probability prediction is generated. Here, we utilize the binaryzation information of density map as the supervision signal to learn semantic information independent of class, and its loss is computed by the binary cross entropy loss defined as follows:

$$\mathcal{L}_a = -\frac{1}{m} \sum_{i=1}^m [b_i \log(q_i) + (1 - b_i) \log(1 - q_i)], \quad (4)$$

where b_i and q_i denote the ground-truth and network prediction, respectively, m denotes the total number of pixels. Note that $q_i = (y_i > \delta)$ where δ is a given threshold.

Despite the fact that we apply the aforementioned supervision signal on this branch, its output will inevitably suffer from prediction inaccuracy. As a result, we invert the output signal before learning it with stacked convolution layers to limit the influence of errors and improve detection of interested foreground and irrelevant regions. Finally, the learned

characteristics and image features are combined to forecast the density map.

C. Support Sample Bank

To address the issue of catastrophe forgetting, this study reviews the old knowledge when acquiring new classes from the perspectives of sample reply and knowledge distillation. Inspired by iCaRL, We follow the principle of rehearsal by selecting representative exemplars from previous classes. Different from these classification-based models, we adopt the features from intermediate convolution layers in regressor as a sample representation. Specifically, we compress the features into a vector through an average pooling layer as the representation of current sample. For each class c_i , we compute a class center by taking the average of the compressed representations of all samples. The samples are then sorted in ascending order based on their distances to their corresponding class center. The top K exemplars are chosen as exemplars from the ranking list and saved as representative counting memory. It should be noted that this study uses fixed-size memory. The quantity of memory samples is then spread evenly across all classes, including background.

As for knowledge distillation, we employ a distillation loss for density map to transfer effective knowledge between current stage and previous stage. Formally, it is formulated as below:

$$\mathcal{L}_{kd} = \frac{1}{2\tilde{n}} \sum_{i=1}^{\tilde{n}} \|z_i^t - z_i^{t-1}\|_2^2, \quad (5)$$

where z_i^{t-1} and z_i^t denote the predicted density estimation by the network from the $(t-1)$ th stage and the t th stage, respectively.

Finally, the overall objective function is given as follows:

$$\mathcal{L}_{total} = \mathcal{L}_a + \mathcal{L}_c + (1 - \lambda)\mathcal{L}_d + \lambda\mathcal{L}_{kd}, \quad (6)$$

where λ is a hyper-parameter. It is worth noting that the distillation loss function \mathcal{L}_{kd} is only employed at incremental phases.

V. EXPERIMENTS

In this section, we perform extensive experiments to illustrate the effectiveness of our proposed network. As a first attempt, we collect an evolving counting dataset for this task, dubbed as EoCo dataset. Then, ablation studies are performed to show the influence of various factors or modules on the proposed model empirically. Further, we conduct the comparison experiments with some existing methods on EoCo dataset. Before presenting the major results, we go over the experimental settings.

A. Implementation Details

Our network is implemented based on the framework of Pytorch. All the experiments are performed on a single NVIDIA RTX 2080Ti GPU. During training, we first resize the images to 400×400 and employ data augmentation strategies such as random flip, random gamma and random graying to avoid over-fitting. We choose the Adam optimizer with weight decay of $5e-5$ to optimize the network parameters. At each incremental stage, we train the network for 300 epochs with batch size 8. The learning rate is initially set to $1e-6$ and reduced by 10 times per 100 epochs. The hyper-parameter λ is loss function is 0.15. As for the ground-truth, we utilize a fixed-size Gaussian kernel, as proposed by MCNN [22], to generate the density map for each sample.

B. EoCo dataset



Fig. 2. Selected examples on EoCo Part A.

As there is no specialized dataset for this task, we introduce a new evolving object counting dataset termed as EoCo, which consists of two parts, Part A and Part B. This is a large-scale

TABLE I
SAMPLE DISTRIBUTION ON EoCo PART A

Class	Train	Val	Test	Total
Person	300 (542.36)	59 (545.59)	182 (433.90)	482
Jujube	201 (74.93)	50 (71.12)	248 (71.22)	499
Cherry	258 (40.90)	50 (43.24)	182 (45.24)	490
Tulip	240 (65.19)	40 (67.35)	215 (66.25)	495
Chicken	220 (44.24)	40 (47.17)	182(46.84)	442
Vehicle	231 (35.81)	44 (34.23)	176 (36.68)	451

TABLE II
SAMPLE DISTRIBUTION ON EoCo PART B

Class	Train	Val	Test	Total
Face	580 (96.45)	60 (93.62)	234 (98.50)	874
Wheat	858 (54.23)	83 (51.87)	372 (53.24)	1313
Person	400 (123.20)	35 (129.71)	316 (124.08)	716
Penguin	740 (70.98)	63 (79.43)	320 (73.21)	1123

dataset with a total of 6885 images, 2859 for Part A and 4026 for Part B, of which 202 are background images. The background set is collected from landscape images, such as grasslands and parks, and does not include any counting objects. On one hand, Part A is divided into six classes: person, jujube, cherry, tulip, chicken and vehicle. Some examples from this part are given in Fig. 2. Among these classes, the training and test of person class are from ShanghaiTech Part A [22], and the rest of the samples is gathered by web crawlers or manual shooting. Note that we randomly select samples from training set for validation due to the lack of validation set in ShanghaiTech Part A. Here we offer standard training, validation and test parts by maintaining the density distribution as nearly consistent as possible. Table I gives a summary of sample distribution in Part A, where we also provide the average density distribution for each class.

On the other hand, we reorganize a dataset Part B with a larger sample size to verify applicability and generalizability of the considered models. All of the samples are from public datasets or competitions, and they are organized into four classes: face [42], wheat [43], person (ShanghaiTech Part B) [22] and penguin [44]. It also include three parts: training, validation and test in which the sample distribution is shown in Table II. Without losing generality, the order of our class increment learning is in accordance with that in the table.

C. Evaluation Metrics

Here we employ the mean absolute error (MAE) and the root mean squared error (MSE) as evaluation metrics. The definitions of the two metrics are presented as follows:

$$MAE = \frac{1}{N} \sum_{i=1}^N |Z_i - \hat{Z}_i| \quad (7)$$

and

$$MSE = \sqrt{\frac{1}{N} \sum_{i=1}^N \|Z_i - \hat{Z}_i\|^2} \quad (8)$$

in which Z_i is the real number of the i th sample, \hat{Z}_i is the predicted number of the i th sample, and N is the total number of samples.

D. Ablation study

To have more insights into our proposed method, we perform ablation studies on the important elements and components on EoCo Part A.

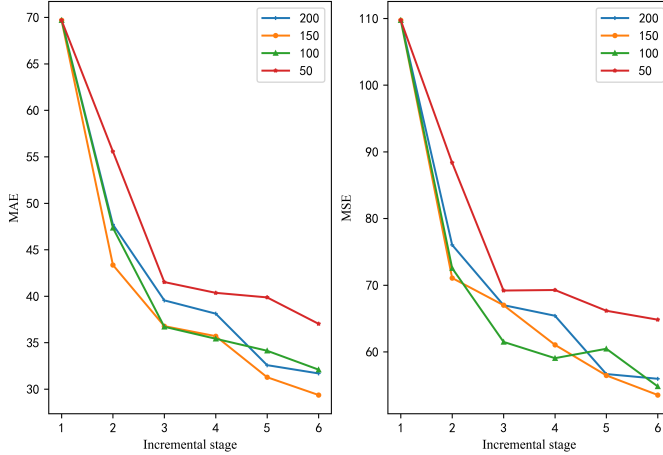


Fig. 3. Visualization and comparison.

(1) Effects of the quantity of memory samples

Memory samples play an important role in recovering old knowledge, of which the quantity also determines the quality of recovery to some extent. Here, we study the effect of the number of memory samples on incremental learning performance, as shown in Fig. 3. From the image, it is clear that the performance, measured in terms of MAE at various incremental stages, decreases noticeably as the number of samples increases from 50 to 150. When at the number of 100 and 150, MSE has some fluctuations from the second stage to the fifth stage. The latter produces a superior performance when it reaches the final stage. However, when the number is increased to 200, the performance is not as good as that of the number 150. We speculate that this may be due to that the class-centered sample selection approach does not take into account the samples of different distributions well, and this sampling approach will only increase samples from a specified density distribution. As a result, the knowledge of other distributions will be easily forgotten in the subsequent learning. Hence, we select 150 as the quantity of memory samples.

(2) Effects of backbone

We explore the effect of different network backbones on incremental models, such as MCNN [22], ResNet [45] and VGG16 [25], as shown in Tables III and IV. Note that we use a three times wider version of MCNN to enrich the feature representation, and aggregate the features from stages 2 and 3 of each ResNet model to enhance the learning of different scale features. From the tables, we can see that the performance of the network keeps getting better as the number of layers deepens, except for VGG16. This again validates

that the deeper networks can extract features with better discriminative information [45]. Obviously, the VGG16-based network outperforms other backbone-based ones while utilizing 13.84 M less parameters than ResNet34 and ResNet50-based networks. This experimentally suggests that VGG16 is more adept at performing the feature extraction for this task. Thus, we choose VGG-16 as the backbone of our network.

(3) Effects of class-agnostic mask module

To show the benefits of class-agnostic mask module, we further conduct additional analysis of the major factors in this module, and then establish the following three baselines:

- **baseline 1** is a basic backbone without class-agnostic mask module to verify the effectiveness of this module.
- **baseline 2** is the version of the original module without supervisory signals. The purpose here is to check if the performance improvement comes from an increase of the number of network parameters.
- **baseline 3** utilizes the density map as a supervision signal instead of the binary mask. This is used to evaluate how different supervision signals affect the network.
- **baseline 4** directly removes the convolutional learning process after mask prediction in this module. This is done to see if the feedback is important to facilitate the two fusion .

The comparison results with these backbones are presented in Table V. We have the following findings: 1) Our method achieves the lowest MAE and MSE at almost all the stages compared to baseline 1. This demonstrates that by learning the generic object occupation prior of different classes, this module can improve network feature representation and lessen the burden of final density regression. 2) We can observe from the comparison with baseline 2 that the performance gain is not due to an increase in the number of network parameters. 3) Interestingly, the findings of baseline 3 show that the density map, as an alternative to the binary mask, also produces good results. This implies that both class-agnostic prior information can assist the network in better mining interested targets, which differs from the findings in [6] for the crowd counting task alone. Nonetheless, we note that the robustness of baseline 3 fluctuates up and down, but the mask-supervised solution exhibits a monotonically decreasing trend as the number of classes grows. 4) The results of baseline 4 show that the single mask supervised signal can hinder density map regression, which is possibly due to the problem of task contradiction between the two supervised signals. In other words, the class increment module seeks to differentiate between various classes, whereas this module maintains consistency in the semantics of different classes. The feedback of mask prediction bridges the gap of two conflicting tasks by the way of simple convolutional learning. In short, this module is able to improve the performance by the rational use of additional signals.

E. Evaluation on EoCo

In this subsection, we will compare with some incremental learning methods to demonstrate the superiority of our method. Since most incremental works are dedicated to classification

TABLE III
ABLATION STUDY ON BACKBONE IN TERMS OF MAE

Backbone	t_0	t_1	t_2	t_3	t_4	t_5	Param (M)
MCNN	126.02	86.83	79.70	62.27	62.61	56.08	4.95
ResNet18	91.70	65.11	52.75	51.49	51.01	48.22	12.85
ResNet34	83.89	51.21	45.14	43.43	51.63	36.24	18.24
ResNet50	80.15	54.79	40.30	38.48	33.89	34.84	27.14
Ours(VGG16)	68.61	43.36	36.78	35.70	31.28	29.37	13.84

TABLE IV
ABLATION STUDY ON BACKBONE IN TERMS OF MSE

Backbone	t_0	t_1	t_2	t_3	t_4	t_5	Param (M)
MCNN	181.71	132.07	124.92	94.63	99.06	92.60	4.95
ResNet18	144.76	103.49	83.15	81.41	78.62	78.26	12.85
ResNet34	130.64	80.19	75.10	69.38	82.22	59.52	18.24
ResNet50	126.64	93.05	71.82	64.04	59.32	55.53	27.14
Ours(VGG16)	107.40	71.08	67.00	61.06	56.47	53.54	13.84

TABLE V
ABLATION STUDY ON CLASS-AGNOSTIC MODULE IN TERMS OF MAE

Model	t_0	t_1	t_2	t_3	t_4	t_5
Baseline 1	73.45	47.50	40.56	34.51	33.90	30.16
Baseline 2	75.59	47.17	39.85	40.58	36.71	31.63
Baseline 3	76.40	43.00	35.23	33.45	34.11	29.20
Baseline 4	78.54	44.06	35.85	34.11	35.34	36.42
Ours	68.61	43.36	36.78	35.70	31.28	29.37

TABLE VI
ABLATION STUDY ON CLASS-AGNOSTIC MODULE IN TERMS OF MSE

Model	t_0	t_1	t_2	t_3	t_4	t_5
Baseline 1	115.87	77.60	66.77	63.20	59.53	51.16
Baseline 2	118.26	71.17	68.73	70.37	63.49	51.51
Baseline 3	121.95	71.30	58.96	60.27	61.07	56.09
Baseline 4	124.73	69.58	58.47	61.11	61.76	61.41
Ours	107.40	71.08	67.00	61.06	56.47	53.54

tasks, we will reproduce their method using the framework of counting tasks. The comparison methods are as follows:

(1) iCaRL [37]. As is mentioned above, iCaRL serves as our baseline 1. It consists of an incremental classifier as well as knowledge distillation and prototype rehearsal for representational learning. In our setup, we also have an incremental regression layer for density map prediction

(2) LwF [36]. Compared to iCaRL, there is no memory available for LwF. New task classifiers and regression layers are trained using examples from new tasks during the training phase, and all classifiers and regression layers are subsequently fine-tuned using the same instances.

(3) Fine-tuning (FT). Following the operation in [46], we fine-tune the whole network after adding a new FC layer and a new regression output.

(4) EEIL [34]. This work proposed a cross-distilled loss in combination with a representative memory component to maintain the knowledge from old classes. In addition, a balanced strategy for fine-tuning was put forward to address the unbalanced training condition.

(5) BiC [47]. Based on the design of this work, we split the exemplars from the old classes and the samples of the new classes into training and validation sets. Then we use

TABLE VII
COMPARISON RESULTS OF INCREMENTAL LEARNING MODELS ON PART A IN TERMS OF MAE

Stage	t_0	t_1	t_2	t_3	t_4	t_5
FT	77.68	74.71	84.56	81.57	69.87	76.42
LwF	84.77	76.05	80.38	83.29	76.25	59.29
iCaRL	73.45	47.50	40.56	34.51	33.90	30.16
EEIL	74.41	47.40	51.92	42.43	44.15	43.32
BiC	68.77	46.20	42.00	43.25	48.23	33.58
Ours	69.70	43.36	36.78	35.70	31.28	29.37
Joint	71.46	40.88	31.92	27.67	25.24	22.11

TABLE VIII
COMPARISON RESULTS OF INCREMENTAL LEARNING MODELS ON PART A IN TERMS OF MSE

Stage	t_0	t_1	t_2	t_3	t_4	t_5
FT	121.32	115.66	132.08	130.32	112.02	123.70
LwF	135.37	118.63	129.41	131.95	126.16	91.84
iCaRL	115.87	77.60	66.77	63.20	59.53	51.16
EEIL	116.67	70.78	89.55	75.55	81.07	73.09
BiC	111.05	70.54	67.86	71.87	84.87	60.24
Ours	109.74	71.08	67.00	61.06	56.47	53.54
Joint	115.05	64.98	52.86	47.56	45.42	38.88

the validation set for bias correction. As there are not enough samples in exemplars, the partition ratio of training/validation here is 2:1.

(6) Joint. The samples from different classes are interleaved to jointly optimize the network parameters. Its performance can be regarded as the upper bound of incremental learning.

We conduct comparative experiments with the above methods on EoCo dataset. To fairly compare these methods, we set the exemplar number to be 150 for rehearsal-based ones. For Part A, the comparison results are summarized in Tables VII and VIII. As shown, the proposed method outperforms these existing incremental methods on two evaluation metrics at almost every stage. Compared to the rehearsal-based methods, LwF and FT do not perform well. It is largely because both methods devote close attention to learning new knowledge and do not retain old knowledge effectively. By comparison, the rehearsal-based methods can better resist catastrophic forgetting by consistently reviewing examples from previous classes. BiC and iCaRL have obtained good results among

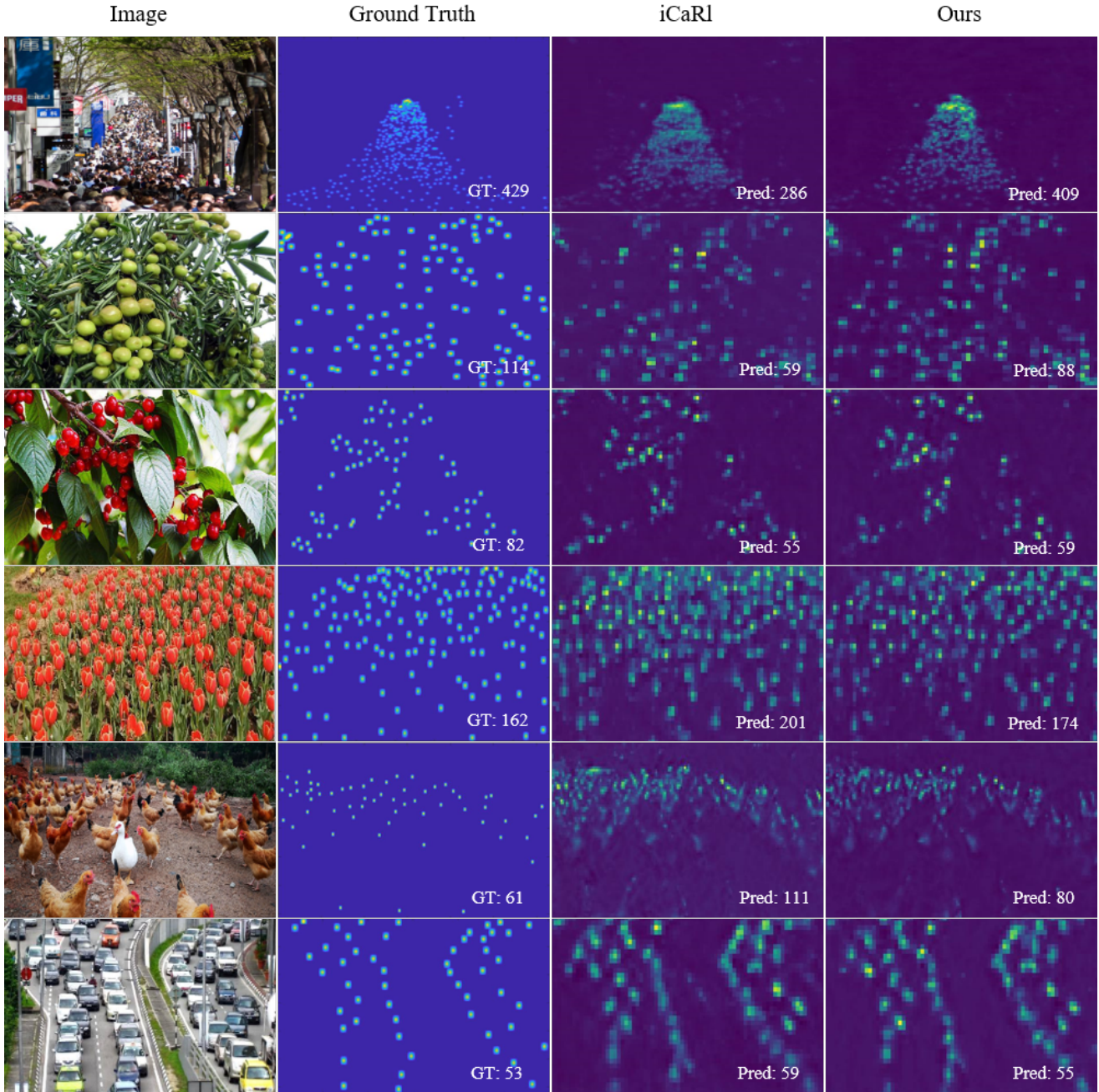


Fig. 4. Visualization results. The first column shows the raw image from the final incremental stage in Part A. The second column shows the ground truth of corresponding image. The last two columns are the estimated density map by iCaRL and our method. The oldest class is at the top, followed by the new class in order.

these rehearsal-based methods. But because BiC is a two-stage training method, training takes more time. Our solution proposes a class-agnostic mask module based on iCaRL to boost the network performance.

As for Part B, the number of each class samples has greatly increased, which greatly increases the difficulty for networks to retain old knowledge under the same exemplars with Part A. We can see from Tables IX and X that our method consistently surpasses the other methods for all incremental training phases. We may get the same conclusion as that in Part A by comparing FT and LwF with the rehearsal-based methods.

Notably, in comparison to iCaRL, our method outperforms it, particularly at the final stage. This demonstrates that our method could mine more discriminative features to achieve a better balance between new knowledge learning and old knowledge retention. In summary, it is simple to conclude that our method is effective at the incremental learning task for crowd counting.

F. Visualization

To further demonstrate the superiority of our method, we compare the estimated density maps of our method to iCaRL at

TABLE IX

COMPARISON RESULTS OF INCREMENTAL LEARNING MODELS ON PART B IN TERMS OF MAE

Stage	t_0	t_1	t_2	t_3
FT	23.20	37.45	27.72	40.08
LwF	28.21	33.94	31.08	46.36
iCaRI	23.62	16.44	14.70	20.60
EEIL	24.57	16.43	18.71	26.39
BiC	23.99	16.99	24.47	28.71
Ours	23.60	16.03	14.19	18.08
Joint	24.08	14.66	13.08	13.97

TABLE X

COMPARISON RESULTS OF INCREMENTAL LEARNING MODELS ON PART B IN TERMS OF MSE

Stage	t_0	t_1	t_2	t_3
FT	55.48	66.17	48.27	65.26
LwF	64.25	59.13	51.47	74.06
iCaRI	55.86	35.55	26.43	34.40
EEIL	57.85	33.87	32.22	39.95
BiC	55.25	32.34	41.24	44.16
Ours	57.02	34.62	25.72	29.12
Joint	56.78	31.56	26.38	25.36

the last incremental stage, as shown in Fig. 4. The figure shows that, in comparison, our method produces more precise count estimation. For instance, in the first image, our method is more accurate than iCaRI in the number estimation of extremely dense crowds. This could be caused by the fact that iCaRI struggles to maintain old information. The similar pattern is evident in other classes. By contrary, our method exhibits higher memory retention and learning capacity.

VI. CONCLUSION

In this study, a propose a unified evolving object counting network for evolving object counting is proposed. It has three components: base net, class incremental module and class-agnostic mask module. The first component aims to extract discriminative features of inputs, the second component serves as a object occupation prior to improve the feature expression capability for better regressing the density map, and the third component implements incremental learning of class-related regressors that are guided online by incremental classifiers. Furthermore, we use knowledge distilling and support sample bank to better retain the old knowledge at the feature and image levels. To complete this goal, we collect a new dataset with different scales that covers common high-density scenarios. Finally, extensive experiments demonstrate the efficacy of our method.

REFERENCES

- [1] S. Zhang, G. Wu, J. P. Costeira, and J. M. Moura, "Understanding traffic density from large-scale web camera data," in *Proceedings of the IEEE Conference on Computer Vision and Pattern Recognition*, 2017, pp. 5898–5907.
- [2] L. Liu, J. Chen, H. Wu, T. Chen, G. Li, and L. Lin, "Efficient crowd counting via structured knowledge transfer," in *Proceedings of the ACM International Conference on Multimedia*, 2020, pp. 2645–2654.
- [3] S. W. Glover and S. L. Bowen, "Bibliometric analysis of research published in tropical medicine and international health 1996–2003," *Tropical Medicine & International Health*, vol. 9, no. 12, pp. 1327–1330, 2004.
- [4] M. Zhao, J. Zhang, C. Zhang, and W. Zhang, "Leveraging heterogeneous auxiliary tasks to assist crowd counting," in *Proceedings of the IEEE/CVF Conference on Computer Vision and Pattern Recognition*, 2019, pp. 12736–12745.
- [5] M. Zhao, C. Zhang, J. Zhang, F. Porikli, B. Ni, and W. Zhang, "Scale-aware crowd counting via depth-embedded convolutional neural networks," *IEEE Transactions on Circuits and Systems for Video Technology*, vol. 30, no. 10, pp. 3651–3662, 2019.
- [6] S. Jiang, X. Lu, Y. Lei, and L. Liu, "Mask-aware networks for crowd counting," *IEEE Transactions on Circuits and Systems for Video Technology*, vol. 30, no. 9, pp. 3119–3129, 2019.
- [7] X. Jiang, L. Zhang, T. Zhang, P. Lv, B. Zhou, Y. Pang, M. Xu, and C. Xu, "Density-aware multi-task learning for crowd counting," *IEEE Transactions on Multimedia*, vol. 23, pp. 443–453, 2020.
- [8] Y. Liu, G. Cao, H. Shi, and Y. Hu, "Lw-count: An effective lightweight encoding-decoding crowd counting network," *IEEE Transactions on Circuits and Systems for Video Technology*, 2022.
- [9] S. Zhang, G. Wu, J. P. Costeira, and J. M. Moura, "Fcn-rlstm: Deep spatio-temporal neural networks for vehicle counting in city cameras," in *Proceedings of the IEEE International Conference on Computer Vision*, 2017, pp. 3667–3676.
- [10] J. Sun, K. Yang, C. Chen, J. Shen, Y. Yang, X. Wu, and T. Norton, "Wheat head counting in the wild by an augmented feature pyramid networks-based convolutional neural network," *Computers and Electronics in Agriculture*, vol. 193, p. 106705, 2022.
- [11] Z. Zhou, Z. Song, L. Fu, F. Gao, R. Li, and Y. Cui, "Real-time kiwifruit detection in orchard using deep learning on android™ smartphones for yield estimation," *Computers and Electronics in Agriculture*, vol. 179, p. 105856, 2020.
- [12] V. A. Sindagi and V. M. Patel, "A survey of recent advances in cnn-based single image crowd counting and density estimation," *Pattern Recognition Letters*, vol. 107, pp. 3–16, 2018.
- [13] G. Gao, J. Gao, Q. Liu, Q. Wang, and Y. Wang, "Cnn-based density estimation and crowd counting: A survey," *arXiv preprint arXiv:2003.12783*, 2020.
- [14] O. Sidla, Y. Lypetsky, N. Brandle, and S. Seer, "Pedestrian detection and tracking for counting applications in crowded situations," in *Proceedings of the IEEE International Conference on Video and Signal Based Surveillance*. IEEE, 2006, pp. 70–70.
- [15] V. B. Subburaman, A. Descamps, and C. Carincotte, "Counting people in the crowd using a generic head detector," in *Proceedings of the International Conference on Advanced Video and Signal-based Surveillance*. IEEE, 2012, pp. 470–475.
- [16] D. Kong, D. Gray, and H. Tao, "Counting pedestrians in crowds using viewpoint invariant training," in *Proceedings of the British Machine Vision Conference*, vol. 1. Citeseer, 2005, p. 2.
- [17] A. B. Chan, Z.-S. J. Liang, and N. Vasconcelos, "Privacy preserving crowd monitoring: Counting people without people models or tracking," in *Proceedings of the IEEE Conference on Computer Vision and Pattern Recognition*. IEEE, 2008, pp. 1–7.
- [18] S.-F. Lin, J.-Y. Chen, and H.-X. Chao, "Estimation of number of people in crowded scenes using perspective transformation," *IEEE Transactions on Systems, Man, and Cybernetics-Part A: Systems and Humans*, vol. 31, no. 6, pp. 645–654, 2001.
- [19] P. F. Felzenszwalb, R. B. Girshick, D. McAllester, and D. Ramanan, "Object detection with discriminatively trained part-based models," *IEEE Transactions on Pattern Analysis and Machine Intelligence*, vol. 32, no. 9, pp. 1627–1645, 2010.
- [20] A. Krizhevsky, I. Sutskever, and G. E. Hinton, "Imagenet classification with deep convolutional neural networks," *Communications of the ACM*, vol. 60, no. 6, pp. 84–90, 2017.
- [21] C. Zhang, H. Li, X. Wang, and X. Yang, "Cross-scene crowd counting via deep convolutional neural networks," in *Proceedings of the IEEE Conference on Computer Vision and Pattern Recognition*, 2015, pp. 833–841.
- [22] Y. Zhang, D. Zhou, S. Chen, S. Gao, and Y. Ma, "Single-image crowd counting via multi-column convolutional neural network," in *Proceedings of the IEEE Conference on Computer Vision and Pattern Recognition*, 2016, pp. 589–597.
- [23] V. A. Sindagi and V. M. Patel, "Generating high-quality crowd density maps using contextual pyramid cnns," in *Proceedings of the IEEE International Conference on Computer Vision*, 2017, pp. 1861–1870.
- [24] Y. Li, X. Zhang, and D. Chen, "Csrnet: Dilated convolutional neural networks for understanding the highly congested scenes," in *Proceedings of the IEEE Conference on Computer Vision and Pattern Recognition*, 2018, pp. 1091–1100.

- [25] K. Simonyan and A. Zisserman, "Very deep convolutional networks for large-scale image recognition," *ArXiv Preprint ArXiv:1409.1556*, 2014.
- [26] U. Sajid, H. Sajid, H. Wang, and G. Wang, "Zoomcount: A zooming mechanism for crowd counting in static images," *IEEE Transactions on Circuits and Systems for Video Technology*, vol. 30, no. 10, pp. 3499–3512, 2020.
- [27] Q. Song, C. Wang, Z. Jiang, Y. Wang, Y. Tai, C. Wang, J. Li, F. Huang, and Y. Wu, "Rethinking counting and localization in crowds: A purely point-based framework," in *Proceedings of the IEEE/CVF International Conference on Computer Vision*, 2021, pp. 3365–3374.
- [28] Y. Tian, X. Chu, and H. Wang, "Cctrans: Simplifying and improving crowd counting with transformer," *ArXiv Preprint ArXiv:2109.14483*, 2021.
- [29] A. Zhang, J. Xu, X. Luo, X. Cao, and X. Zhen, "Cross-domain attention network for unsupervised domain adaptation crowd counting," *IEEE Transactions on Circuits and Systems for Video Technology*, 2022.
- [30] J. Gao, J. Li, H. Shan, Y. Qu, J. Z. Wang, and J. Zhang, "Forget less, count better: A domain-incremental self-distillation learning benchmark for lifelong crowd counting," *arXiv preprint arXiv:2205.03307*, 2022.
- [31] A. K. Nellithimaru and G. A. Kantor, "Rols: Robust object-level slam for grape counting," in *Proceedings of the IEEE/CVF Conference on Computer Vision and Pattern Recognition Workshops*, 2019, pp. 1–9.
- [32] D. Wang, D. Zhang, G. Yang, B. Xu, Y. Luo, and X. Yang, "Ssrnet: In-field counting wheat ears using multi-stage convolutional neural network," *IEEE Transactions on Geoscience and Remote Sensing*, vol. 60, pp. 1–11, 2021.
- [33] E. A. Lins, J. P. M. Rodriguez, S. I. Scoloski, J. Pivato, M. B. Lima, J. M. C. Fernandes, P. R. V. da Silva Pereira, D. Lau, and R. Rieder, "A method for counting and classifying aphids using computer vision," *Computers and electronics in agriculture*, vol. 169, p. 105200, 2020.
- [34] F. M. Castro, M. J. Marín-Jiménez, N. Guil, C. Schmid, and K. Alahari, "End-to-end incremental learning," in *Proceedings of the European Conference on Computer Vision*, 2018, pp. 233–248.
- [35] J. Zhu, B. Luo, S. Zhao, S. Ying, X. Zhao, and Y. Gao, "Iexpressnet: Facial expression recognition with incremental classes," in *Proceedings of the ACM International Conference on Multimedia*, 2020, pp. 2899–2908.
- [36] Z. Li and D. Hoiem, "Learning without forgetting," *IEEE Transactions on Pattern Analysis and Machine Intelligence*, vol. 40, no. 12, pp. 2935–2947, 2017.
- [37] S.-A. Rebuffi, A. Kolesnikov, G. Sperl, and C. H. Lampert, "icarl: Incremental classifier and representation learning," in *Proceedings of the IEEE Conference on Computer Vision and Pattern Recognition*, 2017, pp. 2001–2010.
- [38] A. Chaudhry, M. Ranzato, M. Rohrbach, and M. Elhoseiny, "Efficient lifelong learning with a-gem," in *Proceedings of the International Conference on Learning Representations*, 2019, pp. 1–20.
- [39] O. Tasar, Y. Tarabalka, and P. Alliez, "Incremental learning for semantic segmentation of large-scale remote sensing data," *IEEE Journal of Selected Topics in Applied Earth Observations and Remote Sensing*, vol. 12, no. 9, pp. 3524–3537, 2019.
- [40] S. Yan, J. Xie, and X. He, "Der: Dynamically expandable representation for class incremental learning," in *Proceedings of the IEEE/CVF Conference on Computer Vision and Pattern Recognition*, 2021, pp. 3014–3023.
- [41] U. Michieli and P. Zanuttigh, "Incremental learning techniques for semantic segmentation," in *Proceedings of the IEEE/CVF International Conference on Computer Vision Workshops*, 2019, pp. 1–8.
- [42] S. Yang, P. Luo, C.-C. Loy, and X. Tang, "Wider face: A face detection benchmark," in *Proceedings of the IEEE Conference on Computer Vision and Pattern Recognition*, 2016, pp. 5525–5533.
- [43] "Global wheat detection," <https://www.kaggle.com/competitions/global-wheat-detection>.
- [44] C. Arteta, V. Lempitsky, and A. Zisserman, "Counting in the wild," in *Proceedings of the European Conference on Computer Vision*. Springer, 2016, pp. 483–498.
- [45] K. He, X. Zhang, S. Ren, and J. Sun, "Deep residual learning for image recognition," in *Proceedings of the IEEE Conference on Computer Vision and Pattern Recognition*, 2016, pp. 770–778.
- [46] E. Belouadah and A. Popescu, "Ii2m: Class incremental learning with dual memory," in *Proceedings of the IEEE/CVF International Conference on Computer Vision*, 2019, pp. 583–592.
- [47] Y. Wu, Y. Chen, L. Wang, Y. Ye, Z. Liu, Y. Guo, and Y. Fu, "Large scale incremental learning," in *Proceedings of the IEEE/CVF Conference on Computer Vision and Pattern Recognition*, 2019, pp. 374–382.